Toxicology in Vitro 27 (2013) 2142–2148

Contents lists available at ScienceDirect

Toxicology in Vitro

journal homepage: www.elsevier.com/locate/toxinvit

Impact of iron oxide nanoparticles on brain, heart, lung, liver and kidneys mitochondrial respiratory chain complexes activities and coupling

Yosra Baratli [a,b], Anne-Laure Charles [a], Valérie Wolff [a], Lotfi Ben Tahar [c], Leila Smiri [c], Jamal Bouitbir [a], Joffrey Zoll [a,d], François Piquard [a,d], Olfa Tebourbi [b], Mohsen Sakly [b], Hafedh Abdelmelek [b], Bernard Geny [a,d,*]

[a] Université de Strasbourg, Fédération de Médecine Translationnelle, EA 3072: Mitochondries, Stress oxydant et Protection musculaire, Faculté de Médecine, 67000 Strasbourg, France
[b] Laboratoire de Physiologie Intégrée, Faculté des Sciences de Bizerte, Université de Carthage, 7021 Jarzouna, Tunisia
[c] Unité de recherche UR11ES30, Synthèse et Structures de Nanomatériaux, Faculté des sciences de Bizerte, Université de Carthage, 7021 Jarzouna, Tunisia
[d] Service de Physiologie et d'Explorations Fonctionnelles, Pôle de Pathologie Thoracique, NHC, 67000 Strasbourg, France

ARTICLE INFO

Article history:
Received 28 January 2013
Accepted 9 September 2013
Available online 19 September 2013

Keywords:
Nanoparticles
Ironoxide
Mitochondria
Coupling
Mitochondrial respiratorychain

ABSTRACT

The present study evaluates the effects of iron oxide nanoparticles (ION) on mitochondrial respiratory chain complexes activities in five organs characterized by different oxidative capacities and strongly involved in body detoxification. Isolated mitochondria were extracted from brain, heart, lung, liver and kidneys in twelve Wistar rats (8 weeks) using differential centrifugations. Maximal oxidative capacities (*Vmax*), mitochondrial respiratory chain complexes activity using succinate (*Vsucc*, complexes II, III, and IV activities) or N, N, N′, N′-tetramethyl-p-phenylenediaminedihydrochloride (tmpd)/ascorbate (*Vtmpd*, complex IV activity) and, mitochondrial coupling (*Vmax*/*Vo*) were determined in controls and after exposure to 100, 200, 300 and 500 μg/ml Fe_3O_4. Data showed that baseline maximal oxidative capacities were 26.3 ± 4.7, 48.9 ± 4.6, 11.3 ± 1.3, 27.0 ± 2.5 and 13.4 ± 1.7 μmol O_2/min/g protein in brain, heart, lung, liver, and kidneys mitochondria, respectively. Complexes II, III, and IV activities also significantly differed between the five organs. Interestingly, as compared to baseline values and in all tissues examined, exposure to ION did not alter mitochondrial respiratory chain complexes activities whatever the nanoparticles (NPs) concentration used. Thus, ION did not show any toxicity on mitochondrial coupling and respiratory chain complexes I, II, III, and IV activities in these five major organs.

© 2013 Elsevier Ltd. All rights reserved.

1. Introduction

As a result of their unique physicochemical properties, nanoparticles are becoming present in sunscreens, toothpastes, sanitary ware coatings, and even food products. Currently, researchers are focusing on many areas such as applied physics and chemistry, mechanical and electrical engineering, nanotoxicology, nanobiology and nanomedicine, industrial applications and environmental investigations (Ferreira et al., 2012).

Exploring biomedical uses of nanomaterial, iron oxide nanoparticles (ION) are very interesting. They are used in cell labeling (Chen et al., 2010), drug targeting (Alexiou et al., 2005), gene delivery (McBain et al., 2008), biosensors, hyperthermia therapy and as contrast agents in magnetic resonance imaging (Puppi et al., 2011; Rumenapp et al., 2012).

However, their biological reactivity can be enhanced and can lead to potential toxic interactions. Thus, (Zhu et al., 2010) demonstrated that superparamagnetic iron oxide nanoparticles (SPION) generate injuries in endothelial cells and might play a key role in downstream cardiovascular diseases such as atherosclerosis, hypertension and myocardial infarction. Owing to their ultra-fine sizes, ION can elicit a spectrum of tissue responses including cell activation, generation of reactive oxygen species (ROS), and cell death (Wilson et al., 2002; Zhu et al., 2011).

Abbreviations: NPs, nanoparticles; ION, iron oxide nanoparticles; *Vmax*, maximal oxidative capacities; *Vsucc*, complexes II, III and IV activities; *Vtmpd*, complex IV activity; DEG, diethyleneglycol; ACR, acceptor control ratio.

* Corresponding author at: Université de Strasbourg, Fédération de Médecine Translationnelle, EA 3072: Mitochondries, Stress oxydant et Protection musculaire, Faculté de Médecine, 67000 Strasbourg, France. Tel.: +33 369550879; fax: +33 369551826.

E-mail address: bernard.geny@chru-strasbourg.fr (B. Geny).

0887-2333/$ - see front matter © 2013 Elsevier Ltd. All rights reserved.
http://dx.doi.org/10.1016/j.tiv.2013.09.006

Mitochondria are a main source of ATP production and are particularly involved in the balance between cell survival and cell death. Thus, most cellular energy is obtained through oxidative phosphorylation, a process requiring the action of a set of respiratory enzyme complexes located in the inner mitochondrial membrane, it appears mandatory to study the activities of the different mitochondrial respiratory chain complexes (Horn et al., 2008).

Accordingly, mitochondrial dysfunctions appear as early signs of cells damage in several experimental settings (Charles et al., 2011; Duteil et al., 2010) but mitochondrial implication in ION toxicity remains poorly known and controversial. Indeed, previous studies demonstrated either no mitochondrial damage (Jeng and Swanson, 2006; Xu et al., 2010) or mitochondrial ultrastructural disorganization (Yurchenko et al., 2010; Zhu et al., 2010). Particularly, reports indicated that ION were mainly found in the cytoplasmic vesicles, with no localization in the endoplasmic reticulum, mitochondria and nucleus (Xu et al., 2010). However, even if ION are not localized into mitochondria, these NPs might induce mitochondrial damage. Au et al. (2007) reported that addition of Fe_3O_4 nanoparticles in mature astrocytes induced mitochondrial uncoupling but did not alter cell membrane integrity. Zhu et al. (2010) demonstrated that Fe_3O_4 nanoparticles could generate loss of mitochondria membrane potential. (Karlsson et al., 2008) have shown that subway particles that are composed of a high percentage of magnetite (Fe_3O_4) can cause genotoxicity via mitochondrial depolarisation. Zhu et al. (2011) reported that ION could transfer across the human aortic endothelial cells membrane, localize into vesicles compartments and result in mitochondrial swelling and disappearance of mitochondria.

The deleterious effects of ION are linked to NPs ability to generate oxidative stress. Transition metal nanoparticles like iron may generate ROS (in particular hydroxyl radicals) by acting as catalysts in Fenton-type reactions (Risom et al., 2005). Since besides generating ATP, mitochondria are also a major source of intracellular ROS production, it appeared interesting to investigate mitochondrial respiratory chain complexes activities. Further, one might suppose that difference in oxidative capacities might participate in tissue specificity of NPs deleterious effects. Indeed, (Mahmoudi et al., 2011) recently demonstrated that ION did not produced significant changes on the actin cytoskeleton of heart cells but severely disrupted the actin cytoskeleton in kidneys and brain cells. Such tissue specificity might be related to different detoxification approaches used by the cells for toleration/fight against NPs but, specific oxidative capacities might have played a role. Accordingly, tissue with high oxidative capacity demonstrated reduced ROS production and might be protected against ischemia-reperfusion or statin-related increase in oxidative stress, as compared to tissue with low oxidative capacity (Anderson and Neufer, 2006; Bouitbir et al., 2012; Chan et al., 2004).

The aim of this study was therefore to determine, for the first time, whether Fe_3O_4 nanoparticles might impair mitochondrial respiratory chain in five organs characterized by different oxidative capacities and strongly involved in body detoxification. Thus, we submitted isolated mitochondria harvested from brain, heart, lung, liver and kidneys to different concentrations of Fe_3O_4 nanoparticles (100, 200, 300 and 500 μg/ml) and determined mitochondrial coupling and respiratory chain complexes I, II, III, and IV activities. Indeed, Karlsson et al., 2008 demonstrated that the toxicity of bare iron oxide NPS was absent or very low for human lung epithelial cell line up to concentrations of 100 μg/ml. Jeng and Swanson, 2006 demonstrated that Fe_3O_4 had no measurable effect on the cells until the concentrations reached more than 200 μg/ml and Hussain et al., 2005 showed that Fe_3O_4 had no measurable effect at lower doses (10–50 μg/ml) while there was a significant effect at higher levels (100–250 μg/ml).

2. Material and methods

2.1. Material and reagents

Iron oxide nanoparticles were acquired from unit of UR11ES30, Faculty of science of Bizerte, Tunisia. They were prepared by the polyol process starting from Iron (II) acetate as metal precursor, diethylene glycol (hereafter abbreviated to as DEG) as solvent, purchased from ACROS Organics. All chemicals were used as received without further purification. Deionized water was used in these preparations. For the synthesis of the magnetite (Fe_3O_4) nanoparticles, an appropriate amount of Iron (II) acetate precursor was added to a given volume (125 mL) of DEG to reach nominal iron cations concentration of 0.2 M. The mixture was then refluxed at a rate of +6 °C min^{-1} under mechanical stirring up to boiling point, and then maintained at this temperature for about 2 h. The powders were washed several times with ethanol, then with acetone under ultrasonication with intermittent centrifugation and then dried in air at 50 °C. This iron oxide Fe_3O_4 (magnetite) could be preliminarily distinguished by its black color and their magnetic response when subjected to a permanent magnet.

2.2. Nanoparticle characterization using transmission electron microscopy (TEM)

The size and shape of prepared particles were analyzed on a JEOL-100-CX II Transmission Electron Microscope (TEM) operating at 100 kV equipped with an energy dispersive spectrometer (EDX) (Basti et al., 2010).

2.3. Animals

Twelve male Wistar rats weighing 300–400 g (age 8 weeks) were housed in a thermo-neutral environment (22 ± 2 °C), on a 12:12 h photoperiod, and were provided food and water *ad libitum*. This investigation was carried out in accordance with the Helsinki accords for human treatment of animals during experimentation.

Rats were submitted to general anesthesia with 3% isoflurane and oxygen (1 L/min) in an induction chamber (Minerve, Esternay, France). Anesthesia was maintained with 1.5% isoflurane and 1 L/min oxygen at under spontaneous ventilation. Organs (brain, heart, lung, liver, and kidneys) were excised and cleaned and then immediately used for the study of respiratory parameters (Kindo et al., 2012).

2.4. Extraction of mitochondria

All operations were carried on ice. A piece of tissue was placed into buffer A containing 50 mM tris, 1 mM EGTA, 70 mM Sucrose, 210 mM Mannitol, pH 7.40 at +4 °C. Tissues were finely minced with scissors, placed in buffer A and homogenized with a Potter–Elvehjem. Then, the homogenate was centrifuged at 1300*g* for 3 min, 4 °C. The supernatant was centrifuged at 10,000*g* for 10 min, 4 °C to sediment mitochondria. Finally, the mitochondrial pellet was washed twice and then suspended in 50 mM Tris, 70 mM sucrose, 210 mM mannitol, pH 7.4 at +4 °C. Protein content was routinely assayed with a bradford assay using bovine serum albumin as a standard (Bradford, 1976). Mitochondria were kept on ice and used within 4 h.

2.5. Exposure of mitochondria to nanoparticles

The iron oxide nanoparticles were mixed with a solution of NaCl 9‰. The mixture was then stirred vigorously and sonicated for 60 min to break up aggregates. Particle suspensions were vortexed

Table 1
Number of independent analysis of mitochondrial respiratory chain complexes activities (*Vmax*, *Vsucc* and *Vtmpd*) without or with 100, 200, 300 and 500 μg/ml iron oxide nanoparticles (Fe_3O_4) in brain, heart, lung, liver and kidney.

Mitochondrial respiratory chain complexes					
	Control	100 (μg/ml)	200 (μg/ml)	300 (μg/ml)	500 (μg/ml)
Brain	9	6	6	8	6
Heart	12	8	9	10	8
Lung	10	6	6	7	7
Liver	10	7	6	8	6
Kidney	9	7	6	7	6

immediately before each use. Before measurement, 3 ml of solution M containing 100 mM KCL, 50 mM Mops, 1 mM EGTA, 5 mM Kpi, 1 mg/ml defatted bovine serum albumin (BSA) was added to the oxygraph chambers for 10 min. Then, isolated mitochondria (0.30 mg for brain, heart, liver and kidneys), (0.50 mg for lung) were placed in the oxygraph chambers with 10 mM glutamate and 2.50 mM malate as substrates. The temperature was maintained at +25 °C. Isolated mitochondria of each organ were incubated with different concentrations of Fe_3O_4 (0, 100, 200, 300 and 500 μg/ml) during 30 min at +25 °C.

2.6. Measurement of the mitochondrial respiratory chain complexes activities and mitochondrial coupling

Maximal oxidative capacity (*Vmax*) was measured by adding adenosine diphosphate (ADP). When *Vmax* was recorded, electron flow went through complexes I, III, and IV. Complex I was blocked with amytal (0.02 mM) and complex II was stimulated with succinate (25 mM). Mitochondrial respiration in these conditions allowed determining complexes II, III, IV activities (*Vsucc*). After that, N, N, N′, N′-tetramethyl-p-phenylenediamine dihydrochloride (tmpd, 0.5 mM) and ascorbate (0.5 mM) were added as artificial electron donors to cytochrome c. In these conditions, the activity of cytochrome c oxydase (complex IV) was determined as an isolated step of the respiratory chain (*Vtmpd*) (Zoll et al., 2006). The mitochondrial coupling (coupling of phosphorylation to oxidation) was determined by calculating the acceptor control ratio (ACR), the ratio between ADP-stimulated respiration (*Vmax*) over basal respiration (without ADP) with glutamate and malate as substrate (V_0).

2.7. Statistical analysis

Results are expressed as mean ± SEM. A total of 570 independent analysis of mitochondrial respiration were performed. Each mean value was obtained from 6 to 12 original data arising from the specific organ of the 6–12 different animals involved. The number of analysis for *Vmax*, *Vsucc* and *Vtmpd* are presented in Table 1.

Statistical analyses were performed using one way ANOVA followed by a Tukeypost-test. (GraphPad Prism 5, Graph Pad Software, Inc., San Diego, CA, USA). Statistical significance required a $p < 0.05$.

3. Results

3.1. Nanoparticle characterization using transmission electron microscopy (TEM)

TEM imaging of Fe_3O_4 nanoparticles were performed to confirm primary particle size, obtain a size distribution, and to observe the general morphology of the particles (Fig. 1). The TEM image showed that the powders are constituted by roughly spherical almost nonagglomerated particles. In addition, about 250 particles have been counted for the average particle size and histogram determinations. The calculated average diameter was 9 nm with a SD of 1.6 nm.

3.2. Evaluation of the baseline brain, heart, lung, liver and kidneys mitochondrial respiratory chain complexes activities

The maximal oxidative capacities, *Vmax*, reflecting complexes I, III, and IV activities was the highest in the heart (48.9 ± 4.6 μmol O_2/min/g protein) compared to other organs. Thus, *Vmax* was lower in liver (27.0 ± 2.5 μmol O_2/min/g protein), brain (26.3 ± 4.7 μmol O_2/min/g protein), kidneys (13.4 ± 1.7 μmol O_2/min/g protein) and lung (11.3 ± 1.3 μmol O_2/min/g protein) (Table 2).

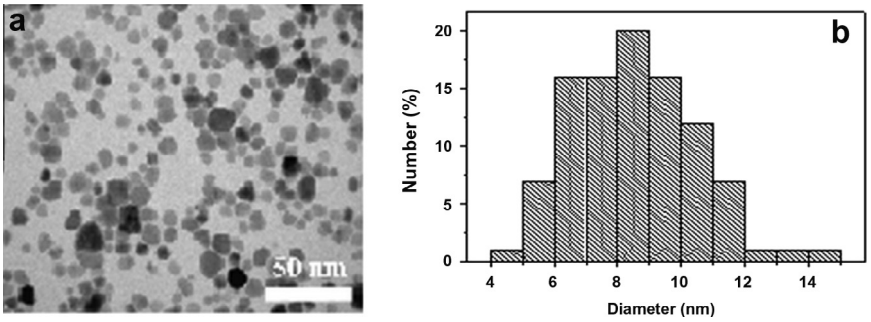

Fig. 1. TEM image (a) and size histogram (b) of the Fe_3O_4 nanoparticles.

Table 2
Baseline brain, heart, lung, liver and kidney mitochondrial respiratory chain complexes activities.

Control	Brain	Heart	Lung	Liver	Kidney
Vmax (μmol O_2/min/g protein)	$26.3 \pm 4.7^{\#\#\#}$	$48.9 \pm 4.6^{\S\S\S £££ ***}$	$11.3 \pm 1.3^{£££}$	$27.0 \pm 2.5^{***}$	13.4 ± 1.7
Vsucc (μmol O_2/min/g protein)	$45.8 \pm 2.9^{\S\S\S}$	$53.9 \pm 4.3^{\S\S\S ££}$	$15.7 \pm 2.0^{£***}$	$33.4 \pm 2.0^{**}$	54.5 ± 4.8
Vtmpd (μmol O_2/min/g protein)	$84.7 \pm 3.6^{\#\S\S\S £££}$	$106.8 \pm 6.2^{\S\S\S £££}$	$24.0 \pm 2.1^{***}$	$42.2 \pm 20.2^{***}$	88.2 ± 8.1

Data are means ± SEM (one-way ANOVA followed by Tukey). $^{\#}p < 0.05$; $^{\#\#}p < 0.01$; $^{\#\#\#}p < 0.001$ vs Heart. $^{\S}p < 0.05$; $^{\S\S}p < 0.01$; $^{\S\S\S}p < 0.001$ vs Lung. $^{£}p < 0.05$; $^{££}p < 0.01$; $^{£££}p < 0.001$ vs Liver. $^{*}p < 0.05$; $^{**}p < 0.01$; $^{***}p < 0.001$ vs Kidney.

Vsucc, reflecting complexes II, III and IV activities, was higher in kidneys (54.5 ± 4.8 μmol O_2/min/g protein), than in heart (53.9 ± 4.3 μmol O_2/min/g protein), brain (45.8 ± 2.9 μmol O_2/min/g protein), liver (33.4 ± 2.0 μmol O_2/min/g protein) and lung (15.7 ± 2.0 μmol/min/g protein) (Table 2).

The *Vtmpd*, reflecting complex IV activity, showed elevated values in heart (106.8 ± 6.2 μmol O_2/min/g protein) compared to other organs. *Vtmpd* was thus lower in kidneys (88.2 ± 8.1 μmol O_2/min/g protein), brain (84.7 ± 3.6 μmol O_2/min/g protein), liver (42.2 ± 2.2 μmol O_2/min/g protein) and lung (24.0 ± 2.1 μmol O_2/min/g protein) (Table 2).

The acceptor control ratio ($Vmax/V_0$), representing the degree of coupling between oxidation and phosphorylation, in controls groups was lower in kidneys (1.7 ± 0.2) as compared to heart (4.5 ± 0.4) and liver (5.7 ± 1.1). Lung and brain ACRs were respectively 3.6 ± 0.6 and 3.2 ± 0.6 (Table 3).

Fig. 2 shows a representative oxygraphic trace with NPs and main mitochondrial substrates.

3.3. Effects of iron oxide nanoparticles on brain, heart, lung, liver and kidneys mitochondrial respiratory chain complexes activities

All data are presented in Figs. 3–7.

Fig. 3 demonstrated that *Vmax*, *Vsucc* and *Vtmpd* were similar without or with exposure to Fe_3O_4 in brain isolated mitochondria.

Similarly, in isolated heart mitochondria, Fe_3O_4 treatment did not alter the mitochondrial function. Concerning the dose of 500 μg/ml, *Vmax* and *Vsucc* (43.7 ± 3.4 vs 48.9 ± 4.6 and 43.4 ± 6.1 vs 53.9 ± 4.3 μmol O_2/min/g protein) were not decreased as compared to controls. Similarly, *Vtmpd* was not decreased as compared to controls but, a significant difference was observed between Fe_3O_4 (200 μg/ml) (118.1 ± 11.0 μmol O_2/min/g protein) and Fe_3O_4 (500 μg/ml) (84.3 ± 8.3 μmol O_2/min/g protein) ($p < 0.05$) (Fig. 4).

In lung isolated mitochondria again, *Vmax*, *Vsucc* and *Vtmpd* were similar without or with exposure to Fe_3O_4. Concerning the dose of 500 μg/ml, *Vmax* and *Vsucc* (10.7 ± 1.7 vs 11.3 ± 1.3 and 15.2 ± 2.9 vs 15.7 ± 2.0 μmol O_2/min/g protein) were not decreased as compared to controls. Similarly, *Vtmpd* was not decreased as compared to controls but, a significant difference was observed between Fe_3O_4 (100 μg/ml) (33.4 ± 1.8 μmol O_2/min/g protein) and Fe_3O_4 (500 μg/ml) (22.8 ± 2.6 μmol O_2/min/g protein) ($p < 0.05$) (Fig. 5). Concerning liver isolated mitochondria, the mitochondrial respiratory function was not modified after Fe_3O_4 nanoparticles exposure. The *Vmax*, *Vsucc* and *Vtmpd* were similar to control values, whatever the ION concentrations used (Fig. 6).

Finally, in kidneys, mitochondrial respiratory function was not affected by exposure to ION. Thus, the high dose of Fe_3O_4 (500 μg/ml), *Vmax* (13.1 ± 2.2 vs 13.4 ± 1.7 μmol O_2/min/g protein), *Vsucc* (47.1 ± 5.1 vs 54.5 ± 4.8 μmol O_2/min/g protein) and the *Vtmpd* (66.8 ± 6.6 vs 88.2 ± 8.1 μmol O_2/min/g protein) remained unchanged compared to control values (Fig. 7).

Concerning the acceptor control ratio (ACR), similar results have been observed and thus, ION did not modified mitochondrial coupling whatever the dose used (Table 3).

Thus globally, whatever the Fe_3O_4 concentration used (from 100 to 500 μg/ml), ION did not alter mitochondrial respiratory chain complexes I, II, III, and IV activities or mitochondrial coupling in these five main organs, as compared to control values.

Table 3
Mitochondrial coupling: controls values and responses to 100, 200, 300 and 500 μg/ml iron oxide nanoparticles (Fe_3O_4) in brain, heart, lung, liver and kidney.

ACR	Brain	Heart	Lung	Liver	Kidney
Control	3.2 ± 0.6	4.5 ± 0.4*	3.6 ± 0.6	5.7 ± 1.1***	1.7 ± 0.2
100 μg/ml	3.2 ± 0.5	4.6 ± 0.5**	3.0 ± 0.5	5.0 ± 0.9**	1.7 ± 0.2
200 μg/ml	3.2 ± 0.7	4.8 ± 0.5	3.4 ± 0.9	5.8 ± 2.3	1.4 ± 0.2
300 μg/ml	3.9 ± 1.0	5.1 ± 0.7	4.4 ± 1.3	5.6 ± 1.3	1.9 ± 0.1
500 μg/ml	3.2 ± 0.7	4.7 ± 0.8*	3.1 ± 0.6	3.3 ± 0.4	2.0 ± 0.3

acceptor control ratio (ACR: *Vmax*/V0). Data are means ± SEM (one-way ANOVA followed by Tukey). *$p < 0.05$; **$p < 0.01$; ***$p < 0.001$ vs Kidney.

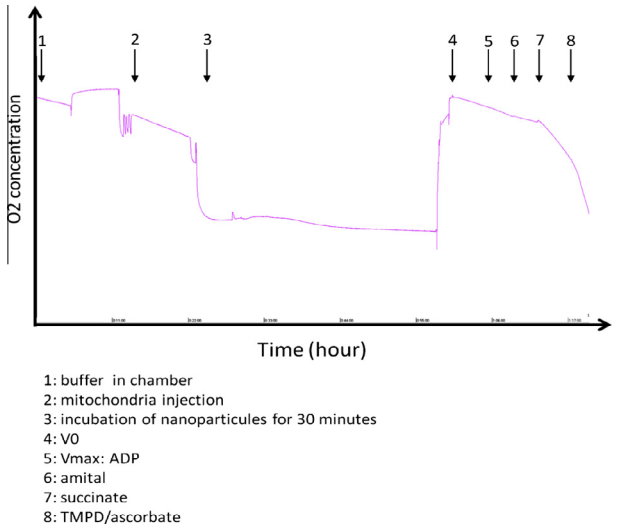

Fig. 2. Representative oxygraphic trace with NPs and main mitochondrial substrates.

4. Discussion

Several studies have shown that intravenously administrated ION can translocate from the blood circulation into various targeted tissues and organs (Corot et al., 2006; Shimada et al., 2006). Nanosized particles can also cross small intestine by persorption and distribute into blood, brain, lung, heart, spleen, liver, kidneys, intestine and stomach (Baroli et al., 2007; Hillyer and Albrecht, 2001; Kwon et al., 2008). Thus, many organs might be exposed through different pathways to potential deleterious effects of ION. Toxic effect of nano-sized complexes on cells depends on material from which they were composed, size, presence of surface reactive groups, concentration, and on cell histogenesis (Karlsson et al., 2009; L'Azou et al., 2008).

In the present study, isolated mitochondria of main organs supporting life and/or involved in detoxification process and characterized by a large span of oxidative capacity (brain, heart, lung, liver and kidneys) were incubated with different concentrations of ION (0, 100, 200, 300 and 500 μg/ml).

Our results are consistent with basal mitochondrial oxidative capacity previously reported. Thus a similar maximal oxidative capacity was observed in the brain, heart and liver (Ling et al., 2012), lung (Freyre-Fonseca et al., 2011) and kidneys (Satav and Katyare, 1982). Further and interestingly, we have demonstrated, for the first time that ION globally failed to impair either mitochondrial respiratory chain complexes activities or coupling in brain, heart, lung, liver and kidneys. Several factors, such as NPs sizes, concentrations, and duration of exposure deserve to be discussed.

NPs size might be important. We chose ION with magnetite (Fe_3O_4) core of 9 nm since ION are used as a remarkable contrast agent that has potential to enhance the evaluation of axillary lymph node metastases in patients with breast cancer (Harada et al., 2007). Li et al. (2012) demonstrated that thermally cross-linked superparamagnetic iron oxide nanoparticles (TCL-SPION) with the same core size of our nanoparticles may be used as a

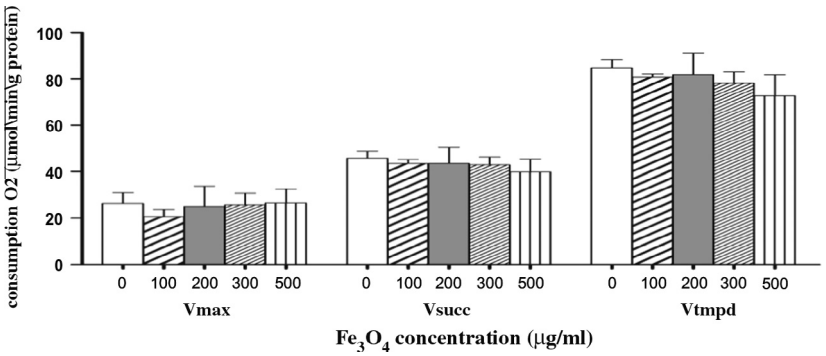

Fig. 3. Effects of iron oxide nanoparticles (Fe_3O_4) on brain liver mitochondrial respiratory chain complexes activities. *Vmax* reflects complexes I, III and I vactivities and is measured using glutamate and malate. *Vsucc* reflects complexes II, III and IV activities and is measured using succinate. *Vtmpd* reflects complex IV activity and is measured using N, N, N′, N′-tetramethyl-p-phenylenediaminedihydrochloride (tmpd) and ascorbate as mitochondrial substrates.

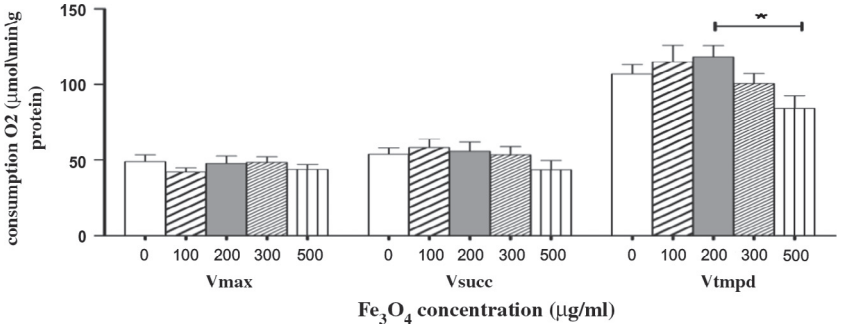

Data are means ± SEM (one-way ANOVA followed by Tukey). * p<0,05 Fe3O4(200µg/ml) vs Fe3O4(500µg/ml).

Fig. 4. Effects of iron oxide nanoparticles (Fe_3O_4) on heart mitochondrial respiratory chain complexes activities. *Vmax* reflects complexes I, III and IV activities and is measured using glutamate and malate. *Vsucc* reflects complexes II, III and IV activities and is measured using succinate. *Vtmpd* reflects complex IV activity and is measured using N, N, N′, N′-tetramethyl-p-phenylenediaminedihydrochloride (tmpd) and ascorbate as mitochondrial substrates.

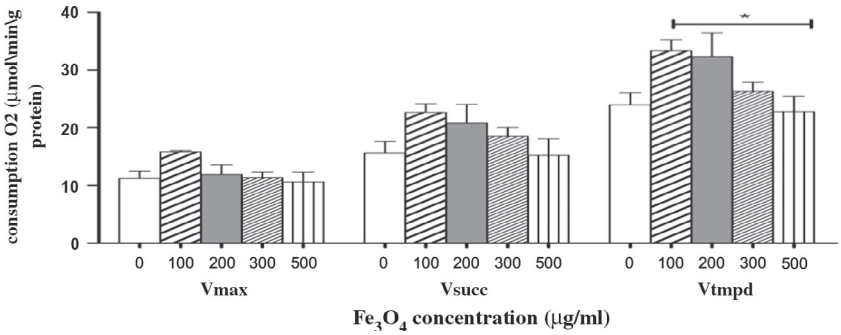

Data are means ± SEM (one-way ANOVA followed by Tukey). * p<0,05 Fe3O4(100µg/ml) vs Fe3O4(500µg/ml).

Fig. 5. Effects of iron oxide nanoparticles (Fe_3O_4) on lung mitochondrial respiratory chain complexes activities. *Vmax* reflects complexes I, III and IV activities and is measured using glutamate and malate. *Vsucc* reflects complexes II, III and IV activities and is measured using succinate. *Vtmpd* reflects complex IV activity and is measured using N, N, N′, N′-tetramethyl-p-phenylenediaminedihydrochloride (tmpd) and ascorbate as mitochondrial substrates.

new platform for tumor imaging and therapy monitoring. (Salnikov et al., 2007) demonstrated that the outer mitochondrial membrane was not permeable to 6-nm particles but 3 nm particles entered the mitochondrial intermembrane space in mitochondria of permeabilized cells and isolated cardiac mitochondria. Thus, our 9 nm ION might have been too big to penetrate isolated mitochondria. We cannot exclude such hypothesis, but as previously reported, NPs can demonstrate mitochondrial toxicity even if they cannot enter into mitochondria (Au et al., 2007).

It was demonstrated that the majority of nanosized complexes revealed their toxic effect on cells at concentrations ranging from 100 to 250 µg/ml (Hussain et al., 2005; Jeng and Swanson, 2006). In the present work, we therefore took care to submit organ mitochondria to such a large span of NPs concentrations. We also examined a concentration of 500 µg/ml, investigating whether a higher concentration might show more toxic effects. It was not the case and thus, concentrations might probably not explain a lack of NPs deleterious effects.

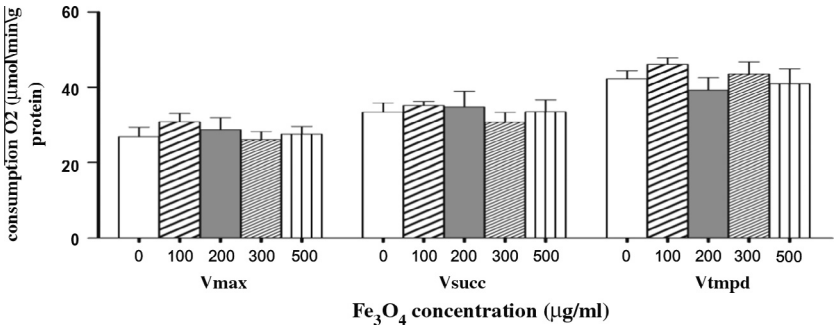

Fig. 6. Effects of iron oxide nanoparticles (Fe_3O_4) on liver mitochondrial respiratory chain complexes activities. *Vmax* reflects complexes I, III and IV activities and is measured using glutamate and malate. *Vsucc* reflects complexes II, III and IV activities and is measured using succinate. *Vtmpd* reflects complex IV activity and is measured using N, N, N′, N′-tetramethyl-p-phenylenediaminedihydrochloride (tmpd) and ascorbate as mitochondrial substrates.

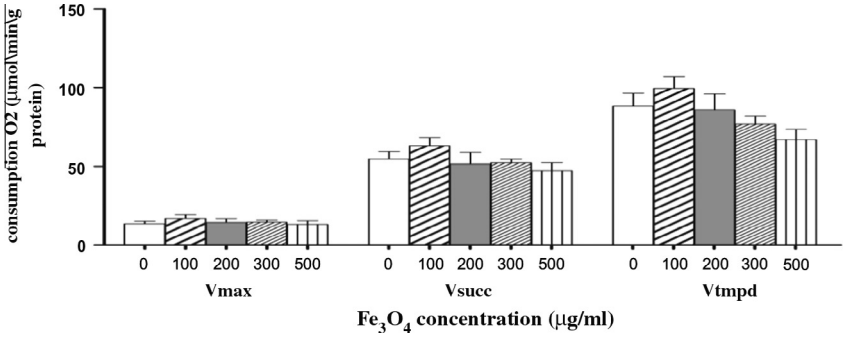

Fig. 7. Effects of iron oxide nanoparticles (Fe_3O_4) on kidney mitochondrial respiratory chain complexes activities. *Vmax* reflects complexes I, III and IV activities and is measured using glutamate and malate. *Vsucc* reflects complexes II, III and IV activities and is measured using succinate. *Vtmpd* reflects complex IV activity and is measured using N, N, N′, N′-tetramethyl-p-phenylenediaminedihydrochloride (tmpd) and ascorbate as mitochondrial substrates.

Concerning duration of exposure, (Buyukhatipoglu and Clyne, 2011) demonstrated that endothelial cell exposure to ION resulted in dose- and time-dependent intracellular ROS formation. ROS formation significantly increased up to an iron oxide concentration of 0.5–1.0 mg/mL and intracellular ROS increased significantly after 2 h of nanoparticle exposure (0.50 mg/mL). The relatively short time of organ exposure to our NPs might thus explain -at least partly- the lack of mitochondrial dysfunction observed in our work. However, it should be noted that in the cited study, both NPs concentrations and size (20–40 nm) were much greater than in our study. Furthermore, incubation period varies widely in published data, ranging from 1 to 24 h in Costa et al., 2010; Hussain et al., 2005 works, respectively. Costa et al., 2010 demonstrated that 1 h incubation was enough for silver nanoparticles to decrease mitochondrial function but since we observed increased ROS production as soon as after 30 min exposure of cardiomyocytes to combined Diltiazem and N-Acetylcystein (Steib et al., 2013), we decided to submit all mitochondria to a 30 min incubation. Indeed, cells are likely to be more resistant to NPs than isolated mitochondria (Freyre-Fonseca et al., 2011).

Complex IV might need a further discussion. Indeed, although we failed to find a significant difference with control values, *Vtmpd* was decreased when comparing Fe_3O_4 (500 µg/ml) and Fe_3O_4 (200 µg/ml) or Fe_3O_4 (100 µg/ml) in heart and lung, respectively. Although this might simply be artifactual, it might alternatively support a specific toxicity of Fe_3O_4 (500 µg/ml) on complex IV of the mitochondrial respiratory chain. Indeed, as reported by Mukhopadhyay et al. (2012) the bare Fe_3O_4 NPs have considerable magnetism at room temperature and his interaction with cytochrome c leads to the reduction of the protein. Moreover, the same treatments altered the redox state of cytochrome c (Kai et al., 2011). Interestingly, the concentration used in the present study was comparable with the highest concentration (0.5 mg/mL).

5. Conclusion

In conclusion, exposure of normal brain, heart, lung, liver and kidneys to 9 nm- sized Fe_3O_4 nanoparticles did not significantly alter their mitochondrial respiratory chain complexes activities or mitochondrial coupling. This suggest that, in this setting, such NPs has no or a very low mitochondrial toxicity. Further investigations would be helpful to determine whether this holds true in case of fragilized mitochondria, as observed during aging or many diseases and whether complexe IV might be more sensitive to Fe_3O_4 at very high concentrations.

Conflict of interest

None.

Acknowledgments

We thank FabienneGoupilleau, Isabelle Bentz and Anne-Marie Kasprowicz for their expert biological and secretarial assistances.

References

Alexiou, C., Tietze, R., Schreiber, E., Lyer, S., 2005. Nanomedicine: magnetic nanoparticles for drug delivery and hyperthermia – new chances for cancer therapy. Bundesgesundheitsblatt Gesundheitsforschung Gesundheitsschutz 53, 839–845.

Anderson, E.J., Neufer, P.D., 2006. Type II skeletal myofibers possess unique properties that potentiate mitochondrial H(2)O(2) generation. Am. J. Physiol. Cell Physiol. 290, C844–C851.

Au, C., Mutkus, L., Dobson, A., Riffle, J., Lalli, J., Aschner, M., 2007. Effects of nanoparticles on the adhesion and cell viability on astrocytes. Biol. Trace Elem. Res. 120, 248–256.

Baroli, B., Ennas, M.G., Loffredo, F., Isola, M., Pinna, R., Lopez-Quintela, M.A., 2007. Penetration of metallic nanoparticles in human full-thickness skin. J. Invest. Dermatol. 127, 1701–1712.

Basti, H., Ben Tahar, L., Smiri, L.S., Herbst, F., Vaulay, M.J., Chau, F., Ammar, S., Benderbous, S., 2010. Catechol derivatives-coated Fe_3O_4 and gamma-Fe_2O_3 nanoparticles as potential MRI contrast agents. J. Colloid Interface Sci. 341, 248–254.

Bouitbir, J., Charles, A.L., Echaniz-Laguna, A., Kindo, M., Daussin, F., Auwerx, J., Piquard, F., Geny, B., Zoll, J., 2012. Opposite effects of statins on mitochondria of cardiac and skeletal muscles: a 'mitohormesis' mechanism involving reactive oxygen species and PGC-1. Eur. Heart J. 33, 1397–1407.

Bradford, M.M., 1976. A rapid and sensitive method for the quantitation of microgram quantities of protein utilizing the principle of protein-dye binding. Anal. Biochem. 72, 248–254.

Buyukhatipoglu, K., Clyne, A.M., 2011. Superparamagnetic iron oxide nanoparticles change endothelial cell morphology and mechanics via reactive oxygen species formation. J. Biomed. Mater. Res. A 96, 186–195.

Chan, R.K., Austen Jr., W.G., Ibrahim, S., Ding, G.Y., Verna, N., Hechtman, H.B., Moore Jr., F.D., 2004. Reperfusion injury to skeletal muscle affects primarily type II muscle fibers. J. Surg. Res. 122, 54–60.

Charles, A.L., Guilbert, A.S., Bouitbir, J., Goette-Di Marco, P., Enache, I., Zoll, J., Piquard, F., Geny, B., 2011. Effect of postconditioning on mitochondrial dysfunction in experimental aortic cross-clamping. Br. J. Surg. 98, 511–516.

Chen, C.L., Zhang, H., Ye, Q., Hsieh, W.Y., Hitchens, T.K., Shen, H.H., Liu, L., Wu, Y.J., Foley, L.M., Wang, S.J., Ho, C., 2010. A new nano-sized iron oxide particle with high sensitivity for cellular magnetic resonance imaging. Mol. Imaging Biol. 13, 825–839.

Corot, C., Robert, P., Idee, J.M., Port, M., 2006. Recent advances in iron oxide nanocrystal technology for medical imaging. Adv. Drug. Deliv. Rev. 58, 1471–1504.

Costa, C.S., Ronconi, J.V., Daufenbach, J.F., Goncalves, C.L., Rezin, G.T., Streck, E.L., Paula, M.M., 2010. In vitro effects of silver nanoparticles on the mitochondrial respiratory chain. Mol. Cell Biochem. 342, 51–56.

Duteil, D., Chambon, C., Ali, F., Malivindi, R., Zoll, J., Kato, S., Geny, B., Chambon, P., Metzger, D., 2010. The transcriptional coregulators TIF2 and SRC-1 regulate energy homeostasis by modulating mitochondrial respiration in skeletal muscles. Cell Metab. 12, 496–508.

Ferreira, A.J., Cemlyn-Jones, J., Robalo Cordeiro, C., 2012. Nanoparticles, nanotechnology and pulmonary nanotoxicology. Rev. Port Pneumol..

Freyre-Fonseca, V., Delgado-Buenrostro, N.L., Gutierrez-Cirlos, E.B., Calderon-Torres, C.M., Cabellos-Avelar, T., Sanchez-Perez, Y., Pinzon, E., Torres, I., Molina-Jijon, E., Zazueta, C., Pedraza-Chaverri, J., Garcia-Cuellar, C.M., Chirino, Y.I., 2011. Titanium dioxide nanoparticles impair lung mitochondrial function. Toxicol. Lett. 202, 111–119.

Harada, T., Tanigawa, N., Matsuki, M., Nohara, T., Narabayashi, I., 2007. Evaluation of lymph node metastases of breast cancer using ultrasmall superparamagnetic iron oxide-enhanced magnetic resonance imaging. Eur. J. Radiol. 63, 401–407.

Hillyer, J.F., Albrecht, R.M., 2001. Gastrointestinal persorption and tissue distribution of differently sized colloidal gold nanoparticles. J. Pharm. Sci. 90, 1927–1936.

Horn, D., Fontanesi, F., Barrientos, A., 2008. Exploring protein–protein interactions involving newly synthesized mitochondrial DNA-encoded proteins. Methods Mol. Biol. 457, 125–139.

Hussain, S.M., Hess, K.L., Gearhart, J.M., Geiss, K.T., Schlager, J.J., 2005. In vitro toxicity of nanoparticles in BRL 3A rat liver cells. Toxicol. In Vitro 19, 975–983.

Jeng, H.A., Swanson, J., 2006. Toxicity of metal oxide nanoparticles in mammalian cells. J. Environ. Sci. Health A Tox. Hazard Subst. Environ. Eng. 41, 2699–2711.

Kai, W., Xiaojun, X., Ximing, P., Zhenqing, H., Qiqing, Z., 2011. Cytotoxic effects and the mechanism of three types of magnetic nanoparticles on human hepatoma BEL-7402 cells. Nanoscale Res. Lett. 6, 480.

Karlsson, H.L., Cronholm, P., Gustafsson, J., Moller, L., 2008. Copper oxide nanoparticles are highly toxic: a comparison between metal oxide nanoparticles and carbon nanotubes. Chem. Res. Toxicol. 21, 1726–1732.

Karlsson, H.L., Gustafsson, J., Cronholm, P., Moller, L., 2009. Size-dependent toxicity of metal oxide particles–a comparison between nano- and micrometer size. Toxicol. Lett. 188, 112–118.

Kindo, M., Gerelli, S., Bouitbir, J., Charles, A.L., Zoll, J., Hoang Minh, T., Monassier, L., Favret, F., Piquard, F., Geny, B., 2012. Pressure overload-induced mild cardiac hypertrophy reduces left ventricular transmural differences in mitochondrial respiratory chain activity and increases oxidative stress. Front Physiol. 3, 332.

Kwon, J.T., Hwang, S.K., Jin, H., Kim, D.S., Minai-Tehrani, A., Yoon, H.J., Choi, M., Yoon, T.J., Han, D.Y., Kang, Y.W., Yoon, B.I., Lee, J.K., Cho, M.H., 2008. Body distribution of inhaled fluorescent magnetic nanoparticles in the mice. J. Occup. Health 50, 1–6.

L'Azou, B., Jorly, J., On, D., Sellier, E., Moisan, F., Fleury-Feith, J., Cambar, J., Brochard, P., Ohayon-Courtes, C., 2008. In vitro effects of nanoparticles on renal cells. Part Fibre Toxicol. 5, 22.

Li, M., Kim, H.S., Tian, L., Yu, M.K., Jon, S., Moon, W.K., 2012. Comparison of two ultrasmall superparamagnetic iron oxides on cytotoxicity and MR imaging of tumors. Theranostics 2, 76–85.

Ling, B., Peng, F., Alcorn, J., Lohmann, K., Bandy, B., Zello, G.A., 2012. D-Lactate altered mitochondrial energy production in rat brain and heart but not liver. Nutr. Metab (Lond) 9, 6.

Mahmoudi, M., Laurent, S., Shokrgozar, M.A., Hosseinkhani, M., 2011. Toxicity evaluations of superparamagnetic iron oxide nanoparticles: cell "vision" versus physicochemical properties of nanoparticles. ACS Nano 5, 7263–7276.

McBain, S.C., Yiu, H.H., Dobson, J., 2008. Magnetic nanoparticles for gene and drug delivery. Int. J. Nanomedicine 3, 169–180.

Mukhopadhyay, A., Joshi, N., Chattopadhyay, K., De, G., 2012. A facile synthesis of PEG-coated magnetite (Fe_3O_4) nanoparticles and their prevention of the reduction of cytochrome c. ACS Appl. Mater. Interfaces 4, 142–149.

Puppi, J., Mitry, R.R., Modo, M., Dhawan, A., Raja, K., Hughes, R.D., 2011. Use of a clinically approved iron oxide MRI contrast agent to label human hepatocytes. Cell Transplant 20, 963–975.

Risom, L., Moller, P., Loft, S., 2005. Oxidative stress-induced DNA damage by particulate air pollution. Mutat. Res. 592, 119–137.

Rumenapp, C., Gleich, B., Haase, A., 2012. Magnetic nanoparticles in magnetic resonance imaging and diagnostics. Pharm. Res. 29, 1165–1179.

Salnikov, V., Lukyanenko, Y.O., Frederick, C.A., Lederer, W.J., Lukyanenko, V., 2007. Probing the outer mitochondrial membrane in cardiac mitochondria with nanoparticles. Biophys. J. 92, 1058–1071.

Satav, J.G., Katyare, S.S., 1982. Effect of experimental thyrotoxicosis on oxidative phosphorylation in rat liver, kidney and brain mitochondria. Mol. Cell Endocrinol. 28, 173–189.

Shimada, A., Kawamura, N., Okajima, M., Kaewamatawong, T., Inoue, H., Morita, T., 2006. Translocation pathway of the intratracheally instilled ultrafine particles from the lung into the blood circulation in the mouse. Toxicol. Pathol. 34, 949–957.

Steib, A., Collange, O., Quessard, A., Levy, F., Zeisser, M., Charles, AL., Oltean, C., Kretz, JG., Geny, B., Borg, J., 2013. Combined intraoperative use of Diltiazem and N-acetylcystein increases myocardial damage and oxidative stress during off-pump cardiac surgery. Int. J. Cardiol., 26. Apr 26. doi:pii: S0167-5273(13)00655-4.

Wilson, M.R., Lightbody, J.H., Donaldson, K., Sales, J., Stone, V., 2002. Interactions between ultrafine particles and transition metals in vivo and in vitro. Toxicol. Appl. Pharmacol. 184, 172–179.

Xu, H., Dai, W., Han, Y., Hao, W., Xiong, F., Zhang, Y., Cao, J.M., 2010. Differential internalization of superparamagnetic iron oxide nanoparticles in different types of cells. J. Nanosci. Nanotechnol. 10, 7406–7410.

Yurchenko, O.V., Todor, I.N., Khayetsky, I.K., Tregubova, N.A., Lukianova, N.Y., Chekhun, V.F., 2010. Ultrastructural and some functional changes in tumor cells treated with stabilized iron oxide nanoparticles. Exp. Oncol. 32, 237–242.

Zhu, M.T., Wang, Y., Feng, W.Y., Wang, B., Wang, M., Ouyang, H., Chai, Z.F., 2010. Oxidative stress and apoptosis induced by iron oxide nanoparticles in cultured human umbilical endothelial cells. J. Nanosci. Nanotechnol. 10, 8584–8590.

Zhu, M.T., Wang, B., Wang, Y., Yuan, L., Wang, H.J., Wang, M., Ouyang, H., Chai, Z.F., Feng, W.Y., Zhao, Y.L., 2011. Endothelial dysfunction and inflammation induced by iron oxide nanoparticle exposure: risk factors for early atherosclerosis. Toxicol. Lett. 203, 162–171.

Zoll, J., Monassier, L., Garnier, A., N'Guessan, B., Mettauer, B., Veksler, V., Piquard, F., Ventura-Clapier, R., Geny, B., 2006. ACE inhibition prevents myocardial infarction-induced skeletal muscle mitochondrial dysfunction. J. Appl. Physiol. 101, 385–391.